Published in final edited form as:
Hypertension. 2012 October ; 60(4): 965–972. doi:10.1161/HYPERTENSIONAHA.112.195214.

MEDULLARY THICK ASCENDING LIMB BUFFER VASOCONSTRICTION OF RENAL OUTER-MEDULLARY VASA RECTA IN SALT-RESISTANT BUT NOT SALT-SENSITIVE RATS

Paul M. O'Connor[1] and **Allen W. Cowley Jr**[2]

[1]Section of Experimental Medicine, Georgia Health Sciences University, Augusta, GA, USA

[2]Department of Physiology, Medical College of Wisconsin, Milwaukee, WI, USA

Abstract

We have previously demonstrated that paracrine signaling occurs between medullary thick ascending limb (mTAL) and the contractile pericytes of outer-medullary vasa recta (VR) termed 'tubular-vascular cross talk'. The aim of the current study was to determine whether tubular-vascular cross talk has a functional effect on vasoconstrictor responses to angiotensin II, and to determine whether this is altered in the Dahl salt-sensitive (SS) rat. Studies were performed on salt-resistant consomic SS.13^{BN} and SS rats using a novel outer medullary tissue strip preparation in which freshly isolated VR within VR bundles were perfused either alone or in combination with nearby mTAL. In VR from SS.13^{BN} rats, angiotensin II (1μM) increased VR bundle intracellular Ca^{2+} concentration ($[Ca^{2+}]_{VR}$) 19±9nM (n=8) and reduced focal diameter in perfused VR by (−20±7%;n=5). In the presence of nearby mTAL however, $[Ca^{2+}]_{VR}$ (−9±8nM; n=8) and VR diameter (−1±4%, n=7) in SS.13^{BN} rats was unchanged by angiotensin II. In contrast, in Dahl SS rats, angiotensin II resulted in rapid and sustained increase in $[Ca^{2+}]_{VR}$ (89±48 n=7;50±24% n=8) and a reduction in VR diameter of (−17±7;n=7 and −11±4%;n=5) in both isolated VR and VR with nearby mTAL, respectively. In VR with mTAL from SS13^{BN} rats, inhibiton of purinergic receptors resulted in an increase in $[Ca^{2+}]_{VR}$, indicating purinergic signaling buffers vasoconstriction. Importantly, our in vitro data were able to predict medullary blood flow responses to angiotensin II in SS and SS.13^{BN} rats *in vivo*. We conclude that paracrine signaling from mTAL buffers angiotensin II vasoconstriction in Dahl salt-resistant SS.13^{BN} rats but not SS rats.

Keywords

HAEMODYMAICS; HYPERTENSION; BLOOD FLOW REGULATION; MICROCIRCULATION; NITRIC OXIDE; PURINERGIC EFFECT; IMAGING

CORRESPONDING AUTHOR: Dr. Allen W Cowley Jr Department of Physiology, Medical College of Wisconsin, 8701 Watertown Plank Rd, Milwaukee, WI, USA 30912 Phone:414 955 8277 Fax: 414-456-6546 cowley@mcw.edu.

Conflict(s) of Interest/Disclosures none

INTRODUCTION

Renal medullary ischemia promotes sodium and water retention and the development of hypertension[1]. The renal outer medulla is perfused by descending vasa recta capillaries (VR) that branch from the efferent arterioles of juxta-medullary glomeruli[2-4]. Unlike most capillary beds, VR are surrounded by numerous pericyte cell bodies that impart contractility, allowing vascular resistance to be altered at the capillary level[3-5]. Dysfunction of paracrine and autocrine signaling within the local outer medullary milieu may result in hyper-sensitivity of the medullary circulation to vasoconstrictor agents, medullary ischemia and the development of hypertension[1].

Angiotensin II has a direct vasoconstrictor action on descending VR. Angiotensin II induced constriction of VR is mediated by activation of pericyte AT_1 receptors and subsequent depolarization of the plasma membrane and Ca^{2+} entry[6, 7]. Despite the direct constrictor effects of angiotensin II on VR, in normotensive rats in vivo, medullary perfusion is relatively insensitive to the vasoconstrictor actions angiotensin II[8]. However, in Dahl salt-sensitive or L-NAME treated Sprague Dawley rats, medullary perfusion is reduced in response to angiotensin II and chronic angiotensin II infusion results in hypertension[9-11]. The enhanced susceptibility of the medullary circulation to small amounts of circulating angiotensin II in these models likely predisposes these animals to the development of hypertension[1, 11].

In a recent study we demonstrated that medullary thick ascending limb (mTAL) tubular elements of salt-resistant consomic SS.13^{BN} rats produce nitric oxide (NO) in response to angiotensin II stimulation, and that this NO can then diffuse to nearby vasa recta pericytes[12]. Importantly, NO production was blunted in mTAL from Dahl SS rats and NO did not diffuse to neighboring pericyte cell bodies unless tissue superoxide levels were reduced with TEMPOL[12]. As NO reduces vascular tone in isolated VR[5, 13, 14], we hypothesized that diffusion of NO from mTAL to nearby VR pericytes may buffer VR constriction to angiotensin II.

In order to test this hypothesis, we first performed studies in acutely anesthetized Dahl salt-sensitive and consomic SS.13^{BN} rats *in vivo* in which outer medullary blood flow responses were determined using laser Doppler flowmetry in response to angiotensin II infusion. To determine whether these responses may be mediated by tubule-vascular crosstalk between mTAL segments and VR, we developed a unique *in vitro* model in which freshly isolated, perfused VR could be stimulated with vasoactive agents either alone or in the presence of mTAL while maintaining their natural anatomical relationships.

Methods

Experimental animals

Studies used 9-13 week old male SS and SS.13^{BN} rats (MCW inbred strains[15]) weighing 250-350g maintained *ad libitium* on water and a purified AIN-76 rodent diet containing 0.4% NaCl (Dyets, Inc. Bethlehem, PA) since weaning in the animal resource center of the Medical College of Wisconsin. All protocols were approved by the Institutional Animal Care Committee.

Solutions

Hanks balanced salt solution (HBSS) was purchased from Invitrogen (Invitrogen, Grand Island, NY) and HEPES (20mM/L) and L-Arginine (100μM) added and pH adjusted to 7.40. Angiotensin II, L-NAME, L-Arginine and Bovine serum albumin were purchased from Sigma (Sigma Pharmaceutical Company, St Louis, MO).

Renal hemodynamic responses to angiotensin II in SS and SS.13^{BN} rats in vivo

Medullary blood flow responses to angiotensin II infusion were determined in acutely anesthetized SS (n=6) and SS.13^{BN} (n=6) rats using laser Doppler flowmetry. Rats were anesthetized with thiobutabarbital (Inactin; Sigma, 60mg/kg/i.p) and prepared as previously described[16]. Mean arterial pressure (MAP), heart rate (HR), total renal blood flow (TRBF) and outer medullary blood flow (OMBF) were recorded throughout the experimental protocol. The experimental protocol consisted of five 20 min. periods. In the first two 20 min. periods, rats received only maintenance infusions (2mL/hr 2% bovine serum albumin (Sigma)). Following the initial two baseline periods, angiotensin II was added to the vehicle infusion so that rats received 25 nmol/min/kg angiotensin II i.v. The angiotensin II infusion was maintained over an additional two 20 min infusion periods. At the conclusion of these periods, the angiotensin II infusion was stopped and a final 20 min recovery period begun in which animals again received only maintenance fluids. At the cessation of the experimental protocol, animals were euthanized with an overdose of sodium pentobarbital. Background OMBF signal was taken as the signal obtained after the cessation of blood flow.

Isolation of outer medullary tubular and vascular segments

Rats were anesthetized with sodium pentobarbital (60mg/kg/i.p), the left kidney flushed with chilled HBSS via retrograde aortic perfusion, and the kidney excised and prepared for microdissection[17]. Vascular bundles containing VR were identified and either cleared of all visible tubular tissue (isolated VR) or tubular tissue was left remaining intact with the natural anatomical relationships preserved (VR with mTAL). Care was taken to ensure that similar populations of VR were used in both isolated VR and VR with mTAL preparations. Specifically, where possible, a portion of a tissue strip would be used for VR + TAL measurements while from a separate portion of the same strip, the VR were isolated. This ensured that the same VR elements were studied in both groups. VR bundles were visually inspected to ensure all mTAL were removed at 40X. Tissue strips containing either isolated VR or VR with mTAL were adhered to coverslips coated with the tissue adhesive Cell-Tak (BD Biosciences, Bedford, MA). Tissue was then allowed to rest in chilled HBSS solution for approximately 30min before being transferred to a heated imaging chamber maintained at 37°C (Warner Instruments, Hamden, CT) and mounted on the stage of an inverted microscope.

Perfusion of descending vasa recta capillaries in vitro

In studies in which VR diameter was determined, VR were perfused at 5nL per minute with HBSS using pulled glass micropipettes. Perfusion of VR was carried out to prevent the tendency of non-perfused VR capillaries to otherwise collapse making it difficult to accurately quantify reductions of vascular diameter in response to stimuli (Figure 1). In addition to allowing us to more easily identify vascular dimensions, perfusion of VR produced luminal pressure which would facilitate observations of vessel dilation.

Determination of buffering capacity of tubules from SS and SS.13^{BN} rats

To determine whether tubular segments buffered angiotensin II-induced vasoconstriction in VR from Dahl SS and SS.13^{BN} rats, vasoconstrictor responses to 1μM angiotensin II were determined in; 1) isolated VR from SS.13^{BN} rats; 2) VR from SS.13^{BN} rats with mTAL; 3) isolated VR from SS rats; 4) VR from SS rats with mTAL. Prior to the experimental protocol, a region of VR in which multiple pericytes could be identified was selected. The upper and lower focal planes in which VR could be identified were then established and recorded using imaging software (MetaMorph; Universal Imaging, Downingtown, PA). In each group, perfused VR were initially superfused with warmed 37°C HBSS for 10min and images of individual perfused VR recorded at 300 seconds and 60 seconds prior to

administration of angiotensin II. The average of these measurements was taken as baseline resting state diameter. The superfusion solution was then rapidly exchanged with HBSS containing 1μM angiotensin II and images recorded at 30, 60 and 300 seconds following exchange of the buffer solution.

Images were captured using a Nikon TE2000 inverted microscope with an X100 oil immersion (numerical aperture 1.45) TIRF objective lens. The signal was detected using a high-resolution digital camera (Photometrics Cascade 512B, Roper Scientific, Tucson, AZ). At each time point, 40 images were taken at ~1.5-2μM distance (distance between upper and lower focal plane divided by 40 optical sections) along the Z plane so that the optimal level of focus could be obtained at any plane using a motorized Z stage controller (Prior Scientific Inc, Rockland, MA) and MetaMorph imaging software. High resolution stacked images were then saved for analysis.

Quantification of vessel diameter

At the time of analysis one to three points were identified in each image corresponding to points in which pericyte cell bodies were present (Figure 2.). The plane of best focus was then identified for each point by scanning through the stacked image and then luminal inner diameter at each point determined using a MetaMorph image calibrated software package. Measurements at each point were repeated in each of the five stacked images corresponding to each of the time points in which images were taken (300, 60 seconds pre-angiotensin II, 30, 60 and 300 seconds post angiotensin II) in a single preparation.

Determination of VR [Ca^{2+}]

VR and VR with mTAL were isolated as for diameter measurements and loaded with the Ca^{2+} sensitive dye, Fura 2, as previously described (see online supplement for details).VR were visualized at 40X and Ca^{2+} determined using Fura-2 AM and Metafluor imaging software (Universal Imaging, Downingtown, PA) (see online supplement for details) Identifiable cell bodies were selected for measurement within each VR bundle to quantify changes in fluorescent intensity.

Data and statistical analysis

In vivo measurements of renal perfusion—The average TRBF, OMBF and MAP measurements over each period were calculated and the responses compared between SS and $SS.13^{BN}$ rats with 2-way repeated measures ANOVA and Bonferroni post-hoc test. Data are expressed as means ± standard error. *Vessel diameters* -Mean vessel diameter at 300 seconds and 60 seconds prior to administration of angiotensin II was taken to equal resting vessel diameter. The response of VR to angiotensin II was then calculated at each of the three time points following administration of angiotensin II (30, 60 and 300 seconds) by dividing the average vessel diameter at each of these time points with resting vessel diameter and the data expressed as % change from rest. All data are expressed as means + standard error. Responses in mTAL of SS and $SS.13^{BN}$ rats were compared with 2-way repeated measures ANOVA using a Bonferroni post-hoc test. *Vasa recta Ca^{2+} concentration*- $[Ca^{2+}]_{VR}$ was calculated at 3 second intervals for 300 seconds following addition of angiotensin II (1μM) to the bath using the formula described (equation 1). Responses between either SS and $SS.13^{BN}$ rats or $SS.13^{BN}$ vehicle treated versus $SS.13^{BN}$ L-NAME (100μM) treated preparations were compared between with 2-Way repeated measures ANOVA. Data are expressed as means ± standard error. All other data were compared by unpaired t-test.

Results

Renal Medullary perfusion in vivo

Prior to angiotensin II infusion, anesthetized MAP was greater in Dahl SS rats (127±6mmHg) compared with SS.13^{BN} rats (103±4mmHg; P<0.05). Baseline TRBF did not differ between Dahl SS (5.8±0.8ml/min) and SS.13^{BN} (5.4±0.4ml/min) rats. Similarly, baseline OMBF did not differ between Dahl SS (60±10 arbitary units) and SS.13^{BN} rats (68±11arbitary units). While MAP tended to increase during the initial 30 mins of infusion, there was no significant effect of intravenous infusion of angiotensin II (25ng/kg/min i.v) on average MAP in either Dahl SS or Dahl SS.13^{BN} rats over the two 30 min infusion periods. Angiotensin II infusion reduced TRBF similarly in both Dahl SS and Dahl SS.13^{BN} rats (Figure 2.b). Importantly, angiotensin II reduced OMBF in Dahl SS rats but not in Dahl SS. 13^{BN} rats (Figure 2.c; **P<0.05)** indicating greater sensitivity of the medullary circulation of Dahl SS rats to the vasoconstrictor actions of angiotensin II compared with salt-resistant SS. 13^{BN} rats.

Vasa recta diameter

Diameter changes in VR were visualized using a X100 oil immersion (numerical aperture 1.45) TIRF objective lens and high resolution images saved for analysis. Figure 3, shows a typical response of VR from SS.13^{BN} rats with nearby mTAL. Changes in VR diameter were determined between 1-3 pericyte cell bodies on each image, as these are the sites of contraction in VR (Figure 3). VR diameter was determined at 30, 60 and 300 seconds following administration of angiotensin II to the bath (Figure 3). Exchange of the vehicle superfusate with bath media containing angiotensin II (1μM) resulted in a rapid vasoconstriction of isolated VR from Dahl SS.13^{BN} rats (20±7%; P<0.05) that was maintained over the 300 second protocol (Figure 4). In VR from SS.13^{BN} rats with mTAL, angiotensin II resulted in an initial vasoconstriction however, this was not maintained and VR diameter was not different from non-stimulated levels at 300 seconds post angiotensin II (Figure 4). In contrast, in Dahl SS rats, angiotensin II resulted in a rapid and sustained reduction in VR diameter in both isolated VR and VR with mTAL (Figure 4) indicating no functional buffering of VR vasoconstriction by mTAL in these animals.

Vasa recta Ca^{2+} levels

VR pericytes contain contractile elements capable of altering VR diameter in response to increased intracellular Ca^{2+} [7]. Baseline $[Ca^{2+}]_{VR}$ (nM) in each experimental protocol is shown in Table 1 and represents the average intracellular Ca^{2+} levels in all cell bodies identified. In VR alone from SS.13^{BN} rats, $[Ca^{2+}]_{VR}$ increased in response to angiotensin II and this increase was maintained over the entire 300 second protocol (Figure 5). Administration of angiotensin II to VR from SS.13^{BN} rats in the presence of nearby mTAL did not significantly increase $[Ca^{2+}]_{VR}$. (Figure 5). The Ca^{2+} response of VR cell bodies in the presence of nearby mTAL to angiotensin II was significantly different to that of VR alone (P<0.05). In VR from Dahl SS rats in the absence of mTAL, $[Ca^{2+}]_{VR}$ increased in response to Angiotensin II (Figure 5). While in contrast to the response in SS.13^{BN} rats, in VR with mTAL from SS rats, $[Ca^{2+}]_{VR}$ levels remained elevated following administration of angiotensin (Figure 5) and this response was not significantly different from that of VR alone.

Role of paracrine signaling agents

In order to test the role of paracrine signaling agents NO and purines in the functional buffering response of mTAL in VR from SS.13^{BN} rats in response to angiotensin II, we pre-treated tissue strips with either the nitric oxide synthase inhibitor L-NAME or purinergic

receptor antagonist suramin (300μM). In the presence of L-NAME, angiotensin II elicited a sustained elevation $[Ca^{2+}]_{VR}$ levels in VR in the absence of mTAL (Figure 6) which was greater than that of vehicle treated VR. While L-NAME did significantly increase $[Ca^{2+}]_{VR}$ at 300 seconds post angiotensin II in VR with mTAL from SS.13^{BN} rats when compared to vehicle treated VR with mTAL (Figure 6.b), significant buffering of VR constriction remained (Figure 6.a). In contrast, Suramin completely abolished the buffering response of mTAL on $[Ca^{2+}]_{VR}$ in tissue from SS.13^{BN} rats (Figure 7.)

Discussion

The major finding of this study is that renal outer medullary thick ascending limb tubular elements (mTAL) buffer angiotensin II induced vasoconstriction in the salt-resistant consomic SS.13^{BN} rats but not Dahl salt-sensitive rats. Medullary blood flow is an important modulator of the renal pressure natriuresis response and altered responsiveness of the medullary circulation to vasoconstrictor agents such as angiotensin II or vasopressin results in medullary ischemia, Na^+ and water retention and the development of hypertension[1, 11] Our current data provide the first functional evidence that paracrine factors released from tubular elements buffer angiotensin II-mediated vasoconstriction in the outer medulla. Importantly, as these buffering responses were observed only in SS.13^{BN} rats but not in Dahl salt-sensitive rats, these data indicate that tubular dysfunction in the Dahl SS rat contributes to enhanced medullary vascular sensitivity and may predispose these animals to the development of hypertension.

The observation that tubular dysfunction in SS rats results in reduced buffering capacity of the renal medullary capillary circulation is an important step forward in our understanding of the development of salt-sensitive hypertension. While the SS rat is a low renin model of hypertension, a number of studies have demonstrated that intra-renal levels of angiotensin II are abnormally high in the high salt fed SS rats[18,19, 20]. Increased local production of angiotensin II within the kidney of SS rats fed a high salt diet then, may lead to enhanced constriction of medullary VR and the development of hypertension in this strain due to reduced tubular buffering of the vasoconstrictor actions of this peptide. Consistent with this hypothesis, we have previously demonstrated that intra-renal infusion of angiotensin II leads to a reduction in MBF and chronic hypertension in SS rats but not in salt-resistant rats[9]. Further, while the current study focused on the response to angiotensin II, other vasoconstrictor agents may also be important in the development of VR constriction and hypertension in SS rats fed a high salt diet *in vivo*. In addition to angiotensin II, we have previously demonstrated that the renal medullary circulation of Dahl SS rats or rats with reduced medullary NO such as the Dahl rat[11] are hypersensitive to a number of vasoconstrictor agents including norepinephrine[21, 22] and vasopressin[23]. As the mechanisms that buffer angiotensin II- induced vasoconstriction in VR are likely shared with other vasoactive agents, it is probable that the mechanism identified in the current study, tubular dysfunction, underlies the hypersensitivity of the medullary circulation of the SS rat to many of these vasoactive agents. Such a phenomenon may also explain the relatively high doses of angiotensin II required to mediate significant vasoconstriction in our studies as *in vivo* smaller elevations of angiotensin II than those utilized in the current study may act synergistically with other vasoconstrictor stimuli to promote vasoconstriction and the development of chronic hypertension in high salt fed SS rats.

The use of the tissue strip preparation with perfusion of the vasa recta has enabled the identification of differences in tubule-vascular cross talk between Dahl SS and SS.13^{BN} rats. Importantly, these *in vitro* data predicted intra-renal blood flow responses in these strains in response to angiotensin II *in vivo*. Numerous studies have attempted to identify the physiological mechanisms underlying the relative insensitivity of the renal medullary

circulation to vasoconstrictor agents such as endothelin, vasopressin and angiotensin II[24]. We have previously shown that within the renal medullary region, Dahl SS are more sensitive to the vasoconstrictor actions of angiotensin II when compared to Brown Norway (BN) rats[9]. In the current study we now demonstrate that medullary blood flow in Dahl SS rats is also more sensitive to the vasocontrictor actions angiotensin II than that of salt-resistant consomic SS.13^{BN} rats (Figure 3). While our *in vivo* data are consistent with the results of our tissue strip preparation, it remains uncertain whether changes in pericyte contractility are capable of mediating changes in medullary blood flow *in vivo* or whether the upstream actions of angiotensin II on arterioles determines the overall response of the medullary circulation. One possibility is that changes in VR resistance as a result of pericyte constriction alters the distribution of blood flow with the renal inner medulla and papilla. Such changes in distribution could have large effects on metabolism and the medullary solute gradient, both of which could affect Na^+ transport and the development of hypertension in this model. Unfortunately, present methodologies do not allow us to distinguish the role of pericyte-mediated changes in vascular resistance from other parts of the vasculature *in vivo*. New approaches allowing gene targeting within specific cell types such as mTAL in rats[25] however have recently become available and will likely allow these issues to be resolved in the future.

In the current study, we first tested the ability of NO to mediate tubular buffering of VR constriction in SS.13^{BN} rats in response to angiotensin II. In agreement with previous findings [13,26] , our data indicate that reduced NOS activity potentiates the contractile response of VR from SS.13^{BN} rats in VR alone. Treatment with L-NAME however did not abolish buffering responses of mTAL in SS.13^{BN} rats. We conclude that while NO may play a role as a paracrine signaling agent between mTAL and VR in SS.13^{BN} rats, other paracrine signaling molecules must also be important.

mTALs are a significant source of extracellular nucleotides in the renal outer medulla [27-29] and Crawford *et al.* have recently shown that VR pericytes express both P2X and P2Y receptors and that these receptors mediate nucleotide evoked changes in VR diameter[30]. Given these data, we tested the potential of purine metabolites as paracrine signaling agents mediating buffering of contractile responses in SS.13^{BN} rats using the P2 receptor antagonist suramin. Our data indicate that purinergic signaling mediates buffering responses by mTAL in SS.13^{BN} rats (Figure 7). In addition to eliminating the buffering response of mTAL, inhibition of P2 receptors reduced basal $[Ca^{2+}]_{VR}$ in VR with mTAL to levels observed in isolated VR (Table 1) suggesting that purinergic signaling from mTAL to VR may result in pre-constriction of VR. Interestingly, Cabral et al recently published a report indicating that ATP release and subsequent activation of P2 receptors is responsible for flow induced NO production in mTAL[31]. When viewed in context with our current results, these data suggest that purinergic signaling may be an important outer-medullary response to increased luminal flow to activate natriuretic and pathways and maintain medullary perfusion. It is intriguing to speculate that possible dysfunction in such mechansims may be an underlying cause of ischemia, Na^+ retention and the development of hypertension in Dahl SS rats. Further studies will be required to investigate this hypothesis and to identify the specific signaling pathways involved. Also, the role of other likely signaling agents include prostaglandin E2 or adenosine since both of these are produced by the mTAL[27, 29, 32, 33] and have been demonstrated to cause vasodilation in isolated VR[5, 13, 34, 35] and need to be investigated.

The advantage of the perfused vasa recta tissue strip preparation utilized in the current study over previous *in vivo* animal models is that in the current study we were able to determine the cellular source of signaling molecules important in buffering the vasoactive actions of angiotensin II. We are able to conclude that mTALs are the source of these paracrine signaling agents as only when mTAL were present did we observed a reduced contractile

response of VR to angiotensin II. We can reject the possibility that cell types were responsible for the buffering actions we observed in SS.13^{BN} rats for a number of reasons. Firstly, we utilized the inner stripe of the outer medulla only for dissection so that S3 segments of the proximal tubule were not present. Secondly, it is easy to identify OMCD in our preparation due to their bumpy heterogeneous cellular appearance and we were careful to exclude these from tissue strips that were studied. Finally, while renal medullary interstitial cells and thin limb were likely present in our preparation, these cell types would also have been present in VR studied in the absence of mTAL in which we did not observe buffering of the vasoconstrictor response.

In addition to functional measurements of VR diameter, we also measured intracellular [Ca^{2+}] in VR bundles as an index of the contractile state of VR. Since, diameter was not measured in these studies we did not perfuse these vessels. Nevertheless, changes in $[Ca^{2+}]_{VR}$ were consistent with the functional changes we observed in perfused VR. Since a key goal of the current study was to maintain as close as possible the natural anatomical relationships between VR and nearby tubular elements we chose to utilize VR bundles over isolated VR to avoid disruption of these relationships. A caveat of this approach is that it is difficult to clearly distinguish abluminal VR pericytes from luminal VR endothelial cells as in non-perfused, grouped vessels such as those used in Ca^{2+} studies the lumen is often unclear. While any clearly identifiable pericytes were selected, within VR bundles we chose to measure changes in intracellular Ca^{2+} concentration from all cell bodies observed, which undoubtedly included endothelial cells as well as pericytes. A potential caveat to this approach is a finding by Pallone *et al.* that in Fura-2 loaded VR, endothelial cells dominated fluorescent[36]. Importantly, we found that we were able to image Ca^{2+} in pericyte cell bodies even when the endothelium remained intact (Figure 1). This observation is supported by published reports in isolated pericyte laden capillaries of the retina [37], and is likely due to a number of factors including an increased loading time for Fura-2 (30mins in Pallone's study versus 1.5 hours the current study), the use of pluronic F-127 to distribute the dye and the highly sensitive camera to image Ca^{2+} in the current studies. Our data indicating that Ca^{2+} is increased by angiotensin II in isolated VR bundles confirm that much of the Ca^{2+} signal obtained is derived from pericytes rather than endothelial cells[36].

Conclusions

By utilizing a novel experimental approach, we were able to demonstrate directly that tubular paracrine signaling buffers angiotensin II induced vasoconstriction in salt-resistant SS.13^{BN} rats but not Dahl SS rats. Our data indicate that purine signaling may be important in buffering the vasoconstrictor actions of angiotensin II in the renal medulla of salt-resistant rats.

Perspectives

Tubular dysfunction of paracrine signaling appears to underlie the enhanced susceptibility of the renal medullary circulation of Dahl SS rats to vasoconstrictor agents. The development of hypertension and renal disease in this strain is important as it significantly advances our understanding of the mechanisms leading to the development of salt-sensitive hypertension. Our data suggest that targeting tubular dysfunction may be of benefit in preventing renal medullary ischemia and the development of hypertension in salt-sensitive populations.

The unique *in vitro* preparation provides an excellent platform for the further identification of the specific signaling agents that mediate tubulovascular cross-talk. Combined with new gene targeting approaches in rats *in vivo*, we hope that these tools will allow us to identify novel therapeutic approaches for the treatment of renal ischemia and salt-sensitive hypertension.

Supplementary Material

Refer to Web version on PubMed Central for supplementary material.

Acknowledgments

Sources of funding This work was funded by NHBLI grants HL-29587 and American Heart Association fellowship 0625793Z.

References

1. Cowley AW Jr. Role of the renal medulla in volume and arterial pressure regulation. Am J Physiol. 1997; 273(1 Pt 2):R1–15. [PubMed: 9249526]
2. Edwards A, Silldforff EP, Pallone TL. The renal medullary microcirculation. Front Biosci. 2000; 5:E36–52. [PubMed: 10833463]
3. Pallone TL, Silldorff EP, Turner MR. Intrarenal blood flow: microvascular anatomy and the regulation of medullary perfusion. Clin Exp Pharmacol Physiol. 1998; 25(6):383–392. [PubMed: 9673811]
4. Pallone TL, Robertson CR, Jamison RL. Renal medullary microcirculation. Physiol Rev. 1990; 70:885–920. [PubMed: 2194225]
5. Pallone TL, Silldorff EP. Pericyte regulation of renal medullary blood flow. Exp Nephrol. 2001; 9:165–170. [PubMed: 11340300]
6. Pallone TL. Transport of sodium chloride and water in rat ascending vasa recta. Am J Physiol. 1991; 261(3 Pt 2):F519–525. [PubMed: 1887911]
7. Rhinehart K, Handelsman CA, Silldorff EP, Pallone TL. ANG II AT2 receptor modulates AT1 receptor-mediated descending vasa recta endothelial Ca2+ signaling. Am J Physiol Heart Circ Physiol. 2003; 284:H779–789. [PubMed: 12424093]
8. Evans RG, Madden AC, Denton KM. Diversity of responses of renal cortical and medullary blood flow to vasoconstrictors in conscious rabbits. Acta Physiol Scand. 2000; 169:297–308. [PubMed: 10951121]
9. Szentivanyi M Jr. Zou AP, Mattson DL, Soares P, Moreno C, Roman RJ, Cowley AW Jr. Renal medullary nitric oxide deficit of Dahl S rats enhances hypertensive actions of angiotensin II. Am J Physiol Regul Integr Comp Physiol. 2002; 283:R266–272. [PubMed: 12069953]
10. Szentivanyi M Jr. Maeda CY, Cowley AW Jr. Local renal medullary L-NAME infusion enhances the effect of long-term angiotensin II treatment. Hypertension. 1999; 33(1 Pt 2):440–445. [PubMed: 9931144]
11. Cowley AW Jr. Mori T, Mattson D, Zou AP. Role of renal NO production in the regulation of medullary blood flow. Am J Physiol Regul Integr Comp Physiol. 2003; 284:R1355–1369. [PubMed: 12736168]
12. Mori T, O'Connor PM, Abe M, Cowley AW Jr. Enhanced superoxide production in renal outer medulla of Dahl salt-sensitive rats reduces nitric oxide tubular-vascular cross-talk. Hypertension. 2007; 49:1336–1341. [PubMed: 17470722]
13. Cao C, Edwards A, Sendeski M, Lee-Kwon W, Cui L, Cai CY, Patzak A, Pallone TL. Intrinsic nitric oxide and superoxide production regulates descending vasa recta contraction. Am J Physiol Renal Physiol. 2010; 299:F1056–1064. [PubMed: 20702600]
14. Edwards A, Cao C, Pallone TL. Cellular mechanisms underlying nitric oxide-induced vasodilation of descending vasa recta. Am J Physiol Renal Physiol. 2010; 300:F441–456. [PubMed: 21084408]
15. Cowley AW Jr. Roman RJ, Kaldunski ML, Dumas P, Dickhout JG, Greene AS, Jacob HJ. Brown Norway chromosome 13 confers protection from high salt to consomic Dahl S rat. Hypertension. 2001; 37(2 Part 2):456–461. [PubMed: 11230318]
16. Nakanishi K, Mattson DL, Gross V, Roman RJ, Cowley AW Jr. Control of renal medullary blood flow by vasopressin V1 and V2 receptors. Am J Physiol. 1995; 269(1 Pt 2):R193–200. [PubMed: 7631893]

17. Mori T, Cowley AW Jr. Renal oxidative stress in medullary thick ascending limbs produced by elevated NaCl and glucose. Hypertension. 2004; 43:341–346. [PubMed: 14718354]
18. De Miguel C, Das S, Lund H, Mattson DL. T lymphocytes mediate hypertension and kidney damage in Dahl salt-sensitive rats. Am J Physiol Regul Integr Comp Physiol. 2010; 298:R1136–1142. [PubMed: 20147611]
19. Kobori H, Ozawa Y, Suzaki Y, Prieto-Carrasquero MC, Nishiyama A, Shoji T, Cohen EP, Navar LG. Young Scholars Award Lecture: Intratubular angiotensinogen in hypertension and kidney diseases. Am J Hypertens. 2006; 19:541–550. [PubMed: 16647630]
20. Kobori H, Nishiyama A, Abe Y, Navar LG. Enhancement of intrarenal angiotensinogen in Dahl salt-sensitive rats on high salt diet. Hypertension. 2003; 41:592–597. [PubMed: 12623964]
21. Szentivanyi M Jr. Zou AP, Maeda CY, Mattson DL, Cowley AW Jr. Increase in renal medullary nitric oxide synthase activity protects from norepinephrine-induced hypertension. Hypertension. 2000; 35(1 Pt 2):418–423. [PubMed: 10642335]
22. Zou AP, Cowley AW Jr. alpha(2)-adrenergic receptor-mediated increase in NO production buffers renal medullary vasoconstriction. Am J Physiol Regul Integr Comp Physiol. 2000; 279:R769–777. [PubMed: 10956233]
23. Yuan B, Cowley AW Jr. Evidence that reduced renal medullary nitric oxide synthase activity of dahl s rats enables small elevations of arginine vasopressin to produce sustained hypertension. Hypertension. 2001; 37(2 Part 2):524–528. [PubMed: 11230329]
24. Evans RG, Eppel GA, Anderson WP, Denton KM. Mechanisms underlying the differential control of blood flow in the renal medulla and cortex. J Hypertens. 2004; 22:1439–1451. [PubMed: 15257161]
25. Jacob HJ, Lazar J, Dwinell MR, Moreno C, Geurts AM. Gene targeting in the rat: advances and opportunities. Trends Genet. 2010; 26:510–518. [PubMed: 20869786]
26. Sendeski M, Patzak A, Pallone TL, Cao C, Persson AE, Persson PB. Iodixanol, constriction of medullary descending vasa recta, and risk for contrast medium-induced nephropathy. Radiology. 2009; 251:697–704. [PubMed: 19366904]
27. Geyti CS, Odgaard E, Overgaard MT, Jensen ME, Leipziger J, Praetorius HA. Slow spontaneous [Ca2+] i oscillations reflect nucleotide release from renal epithelia. Pflugers Arch. 2008; 455:1105–1117. [PubMed: 18026749]
28. Silva GB, Garvin JL. TRPV4 mediates hypotonicity-induced ATP release by the thick ascending limb. Am J Physiol Renal Physiol. 2008; 295:F1090–1095. [PubMed: 18684885]
29. Beach RE, Watts BA 3rd, Good DW, Benedict CR, DuBose TD Jr. Effects of graded oxygen tension on adenosine release by renal medullary and thick ascending limb suspensions. Kidney Int. 1991; 39:836–842. [PubMed: 1648643]
30. Crawford C, Kennedy-Lydon TM, Callaghan H, Sprott C, Simmons RL, Sawbridge L, Syme HM, Unwin RJ, Wildman SS, Peppiatt-Wildman CM. Extracellular nucleotides affect pericyte-mediated regulation of rat in situ vasa recta diameter. Acta Physiol (Oxf). 2011; 202:241–251. [PubMed: 21624094]
31. Cabral PD, Hong NJ, Garvin JL. ATP mediates flow-induced NO production in thick ascending limbs. Am J Physiol Renal Physiol. 2012 [IN PRESS].
32. Lear S, Silva P, Kelley VE, Epstein FH. Prostaglandin E2 inhibits oxygen consumption in rabbit medullary thick ascending limb. Am J Physiol. 1990; 258(5 Pt 2):F1372–1378. [PubMed: 2159722]
33. Bonvalet JP, Pradelles P, Farman N. Segmental synthesis and actions of prostaglandins along the nephron. Am J Physiol. 1987; 253(3 Pt 2):F377–387. [PubMed: 3307455]
34. Silldorff EP, Kreisberg MS, Pallone TL. Adenosine modulates vasomotor tone in outer medullary descending vasa recta of the rat. J Clin Invest. 1996; 98:18–23. [PubMed: 8690791]
35. Silldorff EP, Yang S, Pallone TL. Prostaglandin E2 abrogates endothelin-induced vasoconstriction in renal outer medullary descending vasa recta of the rat. J Clin Invest. 1995; 95:2734–2740. [PubMed: 7769113]
36. Pallone TL, Silldorff EP, Cheung JY. Response of isolated rat descending vasa recta to bradykinin. Am J Physiol. 1998; 274(3 Pt 2):H752–759. [PubMed: 9530185]

37. Kawamura H, Kobayashi M, Li Q, Yamanishi S, Katsumura K, Minami M, Wu DM, Puro DG. Effects of angiotensin II on the pericyte-containing microvasculature of the rat retina. J Physiol. 2004; 561(Pt 3):671–683. [PubMed: 15486015]

Novelty and Significance

1) What is new

In the current study we demonstrate for the first time that mTAL buffer diameter changes in nearby VR in response to angiotensin II in SS.13^{BN} but not salt-sensitive Dahl SS rats.

2) What is relevant

The Dahl SS rat model is a commonly used model of human salt-sensitive hypertension of which the underlying causes remain unknown. Our data indicate that tubular-dysfunction may be the cause of altered vascular responses and the development of hypertension in this model.

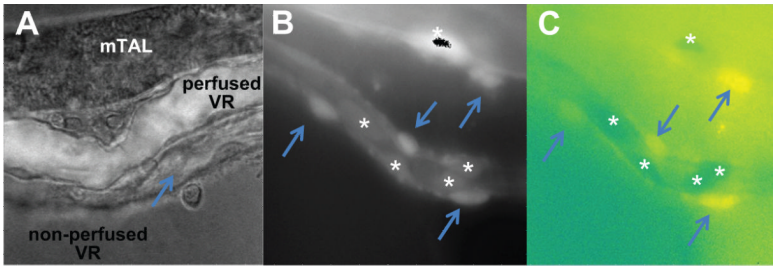

Figure 1.

Shown (a) is an isolated mTAL with VR bundle attached maintaining natural anatomical relationships. A single VR is perfused at 5nL/min with HBSS containing FITC (over-layed image for contrast). Other collapsed VR can be seen in the non perfused state. Shown in (b) a typical Fura-2 loaded VR bundle at EX380/EM510. Fluorescence signal can be observed clearly in both abluminal pericyte (arrows) and intraluminal endothelial cell bodies (*). In (c) the ratio of EX380/EX340 of the same image is shown in pseudo-color. Differences in baseline Ca^{2+} can be observed between un-stimulated pericytes (yellow) and endothelial cells with reduced basal intracellular Ca^{2+} levels (dark green).

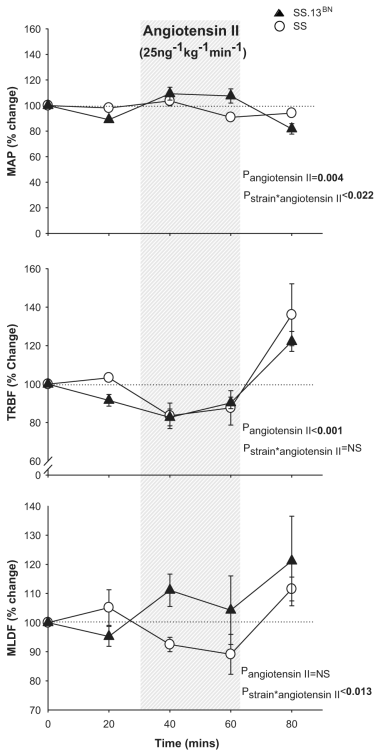

Figure 2.

Mean arterial pressure and renal hemodynamic responses to intra-venous angiotensin II in Dahl SS and SS.13^{BN} rats in vivo. Responses of mean arterial pressure (MAP), total renal blood flow (TRBF) and renal medullary laser Doppler flux (OMBF) in response to intravenous infusion of angiotensin II (25ng.kg^{-1}.min^{-1}) in 0.4%NaCl fed anesthetized Dahl salt sensitive (n=6) and salt-resistant SS.13^{BN} rats (n=6). x axis, time mins; y axis, % change relative to initial 30 min vehicle infusion period; open circles, Dahl salt-sensitive rats; closed triangles, SS.13^{BN} rats; shaded panel, time in which angiotensin II was infused (25ng.kg^{-1}.min^{-1}). Data are mean ± SE. Baseline MAP, TRBF and OMBF values during the initial 30 min vehicle infusion for the Dahl SS group were 129±7mmHg, 5.7±0.8mL/min and 59±11AU and for the SS.13^{BN} group 110±5mmHg, 5.6±0.4mL/min and 67±9AU.

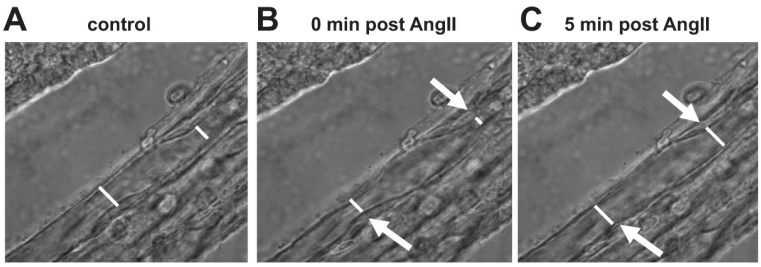

Figure 3.

Determination of VR lumen diameter response to angiotensin II. Perfused VR ($5nL.min^{-1}$) were imaged at 100X using a TIRF 1.45NA oil immersion objective lens. Images in which the inner luminal walls were in clear focus were used for analysis. 2-3 points within each VR corresponding to the location of pericyte cell bodies were identified and the luminal diameter at each point determined prior to- and following administration of angiotensin II to the bath. White lines represent calibrated inner luminal diameter measurements in a) untreated VR, b) VR following administration of angiotensin II (1μM). Arrows indicate areas of focal constriction around pericyte cell bodies in response to angiotensin II.

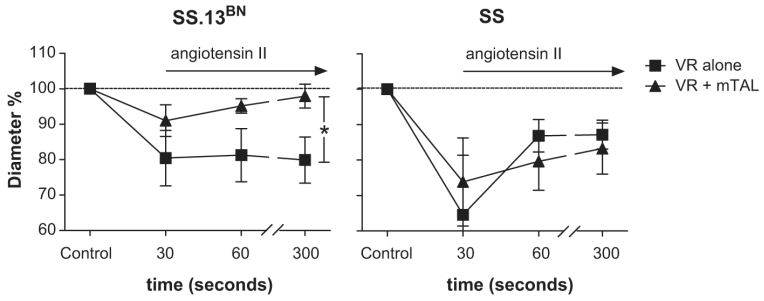

Figure 4.

Vasoconstrictor responses in Dahl SS (n=7 and 5 for isolated VR and VR with mTAL, respectively) and SS.13^{BN} (n=5 and 7 for isolated VR and VR with mTAL, respectively) outer medullary vasa recta to angiotensin II in the presence and absence of nearby nephron segments. The response of *in vitro* perfused VR from Dahl SS.13^{BN} rats (left panel) and Dahl SS rats (right panel) is shown. x axis, time (mins) after administration of angiotensin II (1μM) to the bath media; y axis, % change in VR inner luminal diameter relative to mean of initial VR diameter measurements at 5min and 1min prior to angiotensin II administration (time=control); circles, isolated VR; squares, VR with nearby mTAL; Data are mean ± SE. *, $p<0.05$ for interaction between strain and response to angiotensin II by repeated measures ANOVA.

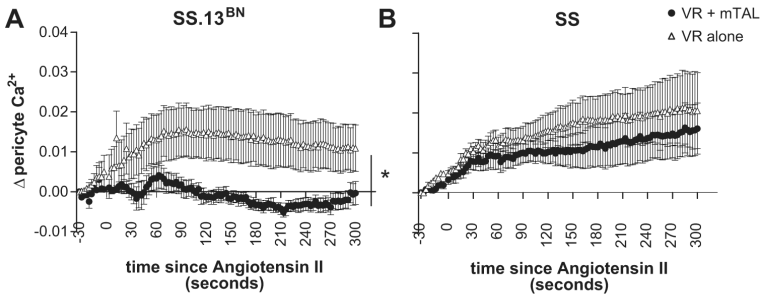

Figure 5.

Intracellular pericyte Ca^{2+} levels from Dahl SS and SS.13^{BN} rats with or without mTAL in response to angiotensin II. The response of VR from Dahl SS.13^{BN} rats (left panel) and Dahl SS rats (right panel) is shown. x axis, time (seconds) after administration of angiotensin II (1μM) to the bath media; y axis, Δ pericyte intracellular calcium levels ($[Ca^{2+}]_{VR}$) in response to angiotensin II as determined by Fura-2 measurement relative to baseline (average of 100 seconds prior to angiotensin II administration). open triangles, VR alone; closed circles, VR with mTAL. Data are mean ± SE. *, $p<0.05$ for interaction between strain and response to angiotensin II by repeated measures ANOVA.

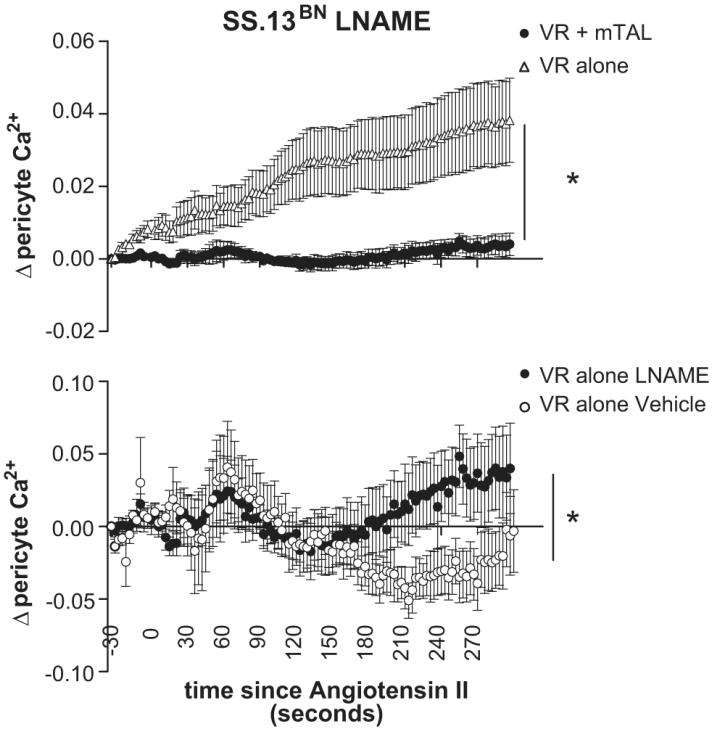

Figure 6.

Effect of nitric oxide synthase inhibition on tubular vascular cross talk response from SS.13^{BN} rats. Intracellular pericyte Ca^{2+} levels from consomic SS.13^{BN} rats with (closed circles) or without mTAL (open circles) in response to angiotensin II pretreated with the nitric oxide synthase inhibitor L-NAME (100μmol/L) are shown (upper panel). Note: L-NAME treatment significantly enhanced Ca^{2+} response to angiotensin II in VR alone compared to vehicle response shown in Figure 5. Response of intracellular pericyte Ca^{2+} levels to angiotensin II from consomic SS.13^{BN} rats with mTAL in either in the presence of the nitric oxide synthase inhibitor L-NAME (closed circles) or vehicle (open circles) are shown (lower panel). x axis, time (seconds) after administration of angiotensin II (1μM) to the bath media; y axis, Δ pericyte intracellular calcium levels ($[Ca^{2+}]_{VR}$) in response to angiotensin II as determined by Fura-2 measurement relative to baseline (average of 100 seconds prior to angiotensin II administration). open triangles, VR alone; closed circles, VR with mTAL. Data are mean ± SE. *, $p<0.05$ for interaction between treatment and response to angiotensin II by repeated measures ANOVA.

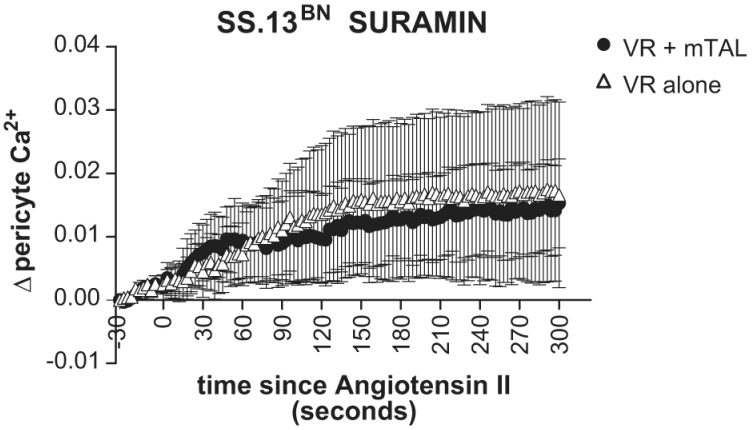

Figure 7.

Effect of P2 receptor inhibition by suramin on tubular vascular cross talk response from SS.13^{BN} rats. Legend as for figure 6.a.

Table 1

Baseline VR cell body intracellular Ca^{2+} concentration $[Ca^{2+}]_{VR}$ (nM) and VR diameter (μM) prior to administration of angiotensin II are shown in table 1. Baseline $[Ca^{2+}]_{VR}$ represents the mean calculated Ca^{2+} concentration from Fura-2 indicator measurments of regions of interest containing pericytes and endothelial cells over a 30 second period prior to administration of angiotensin II. Baseline VR diameter was determined as the mean inner luminal diameter at points between adjacent pericyte cell bodies in individual 300 seconds and 60 seconds prior to administration of angiotensin II. Diameter was measured at 1-3 points along each VR studied and the same points used for subsequent diameter measurements following angiotensin II administration. Images in which the best focus was obtained of the section of the VR of interest from multiple images in a Z stack were used for measurement of diameter. Comparisons were made comparing resting $[Ca^{2+}]_{VR}$ between VR alone and VR with mTAL within the same strain and between strains using students t-test.

Group	Resting diameter (μM)	Resting $[Ca^{2+}]_{VR}$ (nM)
Isolated VR from SS.13 ^{BN}	8.6±1.2 (n=5)	69±14 (n=7)
VR with mTAL from SS.13 ^{BN}	8.8±0.8(n=5)	144±28 (n=8) *
Isolated VR from SS	10.7±1.1 (n=5)	80±31 (n=6)
VR with mTAL from SS	7.8±1.0(n=7)	101±10 (n=8)
Isolated VR from SS.13 ^{BN} **(L-NAME 10μM)**	Not determined	87±50 (n=7)
VR with tubules from SS.13BN (L-NAME 10μM)	Not determined	78±36 (n=7)
Isolated VR from SS.13 ^{BN} **(Suramin 300μM)**	Not determ ined	63±31 (n=6)
VR with tubules from SS.13BN (Suramin 300μM)	Not determined	76±14 (n=5)

* $p<0.05$